



RESEARCH LETTER

10.1029/2021GL095369

From Bright Windows to Dark Spots: Snow Cover Controls Melt Pond Optical Properties During Refreezing

P. Anhaus¹ , C. Katlein¹ , M. Nicolaus¹ , M. Hoppmann¹ , and C. Haas^{1,2} ¹Alfred-Wegener-Institut Helmholtz-Zentrum für Polar- und Meeresforschung, Bremerhaven, Germany, ²Institute of Environmental Physics, University of Bremen, Bremen, Germany

Key Points:

- Refrozen melt ponds may collect a thicker snow cover compared to bare sea ice due to their recessed topography
- Such snow-covered melt ponds transmit less light compared to bare ice of similar type
- This scenario has not been documented before and should be accounted for in studies involving light in a refreezing Arctic Ocean

Supporting Information:

Supporting Information may be found in the online version of this article.

Correspondence to:

P. Anhaus,
philipp.anhaus@awi.de

Citation:

Anhaus, P., Katlein, C., Nicolaus, M., Hoppmann, M., & Haas, C. (2021). From bright windows to dark spots: Snow cover controls melt pond optical properties during refreezing. *Geophysical Research Letters*, 48, e2021GL095369. <https://doi.org/10.1029/2021GL095369>

Received 26 JUL 2021

Accepted 10 NOV 2021

Abstract Melt ponds have a strong impact on the Arctic surface energy balance and the ice-associated ecosystem because they transmit more solar radiation compared to bare ice. In the existing literature, melt ponds are considered as bright windows to the ocean, even during freeze-up in autumn. In the central Arctic during the summer-autumn transition in 2018, we encountered a situation where more snow accumulated on refrozen melt ponds compared to the adjacent bare ice, leading to a reduction in light transmittance of the ponds even below that of bare ice. Results from a radiative transfer model support this finding. This situation has not been described in the literature before, but has potentially strong implications for example on autumn ecosystem activity, oceanic heat budget, and thermodynamic ice growth.

Plain Language Summary Arctic sea ice is covered with snow during autumn, winter and spring. During summer, melt ponds evolve in response to surface melting. After snow fall starts again in autumn, these ponds can be filled with a lot of snow compared to bare ice because of their recessed surface. Indeed, during an expedition close to the North Pole in summer and autumn 2018, we measured a thick snow cover on ponds. This thick snow cover reduced the light availability underneath the ponds to levels below that underneath adjacent bare ice. This is a surprising finding, because it is different from the established theory of high light availability underneath melt ponds during both summer and autumn and how this is described in most computer models. It has consequences for our understanding of the ice-associated ecosystem (organisms that live in and under sea ice). It might also impact the mass and energy balance of central Arctic sea ice during summer-autumn transition when new sea ice starts forming.

1. Introduction

During autumn, winter, and spring, snow controls the optical properties and, thus, regulates the energy as well as the mass balance of sea ice because of its high reflectivity (Grenfell & Maykut, 1977) and insulation (e.g., Sturm et al., 1997). The snow cover of Arctic sea ice is highly variable in time and space (Webster et al., 2014, 2018). The rougher the sea ice topography the more snow accumulates (Massom et al., 1997; Sturm et al., 2002), for example, at the lee sides of pressure ridges (Webster et al., 2018), at windward sides of snow dunes (Dadic et al., 2013), and within the depression of melt ponds (Perovich et al., 2003). In turn, the distribution of snow, especially snow dunes, influences melt pond formation (Petrich et al., 2012; Polashenski et al., 2012). Melt ponds also play a key role for the surface energy budget (Nicolaus et al., 2012) and the mass balance of sea ice (Flocco et al., 2015), as well as for the ice- and ocean-associated ecosystem (Arrigo, 2014). In general, in August-September, the melt pond coverage peaks (Perovich et al., 2002) and open and mature ponds evolve toward refrozen and snow-covered ponds (Perovich et al., 2009). The areal fraction of melt ponds on Arctic first-year ice is up to 53% and 20%–38% on multi-year ice (e.g., Fetterer & Untersteiner, 1998; Nicolaus et al., 2012; Perovich et al., 2003; Webster et al., 2015). This fraction has been shown to increase from 15% to 35% for multi-year ice based on observations from 1994 to 2005 (Perovich et al., 2009) and from 11% to 34% for the entire Arctic based on model simulations from 1996 to 2012 (Schröder et al., 2014). The amount of radiation that is reflected back to the atmosphere is significantly reduced for melt ponds compared to bare ice (e.g., Nicolaus et al., 2012). Instead, a considerable amount of radiation is absorbed by and transmitted through melt ponds (e.g., Ehn et al., 2011; Katlein et al., 2015; Light et al., 2008, 2015; Nicolaus et al., 2012). Consequently, the ice underlying the melt ponds warms and can thin faster than bare ice during summer when no snow is present (Flocco et al., 2015; Hanson, 1965; Untersteiner, 1961).

© 2021. The Authors.

This is an open access article under the terms of the [Creative Commons Attribution License](https://creativecommons.org/licenses/by/4.0/), which permits use, distribution and reproduction in any medium, provided the original work is properly cited.

The translucent melt ponds are often considered as bright windows in Arctic sea ice, even during autumn when their surface refreezes. The formation and occurrence of under-ice phytoplankton blooms are highly dependent on the under-ice light field and, thus, on snow and sea ice conditions (Ardyna et al., 2020). An Arctic-wide increase in the occurrence of the blooms was partly explained by the increasing fraction of melt ponds (Horvat et al., 2017). Lee et al. (2011) showed that ice algal masses accumulate in and under refrozen and snow-free melt ponds that favor higher light availability. They argue that algal accumulations in autumn can provide an important food source for higher trophic animals before and during winter.

This study documents a situation where a thicker snow cover accumulates on melt ponds compared to bare ice after snow fall starts in autumn. The thicker snow cover reduces the light availability under melt ponds to levels lower than under adjacent bare ice. Using data collected in the central Arctic close to the geographic North Pole during the transition from summer to autumn in 2018, we investigate the effect of snow accumulated on the refrozen melt ponds on the under-ice light availability. We compare two datasets that represent the summer and autumn conditions, which mainly consist of snow depth and ice thickness measurements, along with aerial images and under-ice transmittance data from a remotely operated vehicle (ROV). We apply a radiative transfer model to calculate an estimate for the snow accumulation threshold necessary for the light level to be lower under melt ponds compared to bare ice.

2. Materials and Methods

2.1. Study Site

The data presented in this study were collected during the Arctic Ocean 2018 MOCCHA–ACAS–ICE campaign (short: AO18) onboard the Swedish icebreaker *Oden*. During this campaign, a temporary ice camp was set up on drifting, ponded multi-year ice close to the geographic North Pole between 14 August and 14 September 2018. Snow depth, total sea ice thickness (ice thickness plus snow depth), and transmitted irradiance were measured in an area of approximately 100×100 m (Figure 1). Marker poles (M0 to M23) were deployed under the ice to facilitate ROV navigation and to obtain a better co-location of the data. The mean ice thickness of bare ice was 1.9 m and of the ice underlying the melt ponds 1.7 m (Table S2 in Supporting Information S1). Melt ponds were on average 0.3 m deep. Here we focus on two main datasets: measurements performed between 17 and 24 August represented summer conditions which were characterized by open or only slightly refrozen melt ponds and no snow cover, whereas measurements performed between 13 and 14 September represented autumn conditions which were characterized by refrozen and snow-covered melt ponds.

2.2. Snow Depth and Sea Ice Thickness

Snow depth point measurements with a horizontal spacing of 1–3 m and an accuracy of 0.01 m were obtained on the (pristine) study area using a Magna Probe (Snow-Hydro, Fairbanks, AK, USA, Sturm & Holmgren, 2018). On snow-covered bare ice, the Magna Probe likely penetrated into the underlying surface scattering layer (SSL) leading to an overestimate in snow depth. The GPS position of each measurement was recorded by an integrated GPS with an accuracy of 2.5 m (Sturm & Holmgren, 2018).

Total (sea ice plus snow) thickness was determined using a ground-based electromagnetic induction sounding device (GEM-2, Geophex Ltd, Raleigh, NC, USA, Hunkeler, 2016; Hunkeler et al., 2016) using the in-phase signal at a frequency of 18.33 kHz. The GEM-2 was placed on a sled and dragged across the study area in a grid pattern at the very end of the campaign. The accuracy of the total thickness measurements is ± 0.1 m (Hunkeler, 2016; Hunkeler et al., 2016). Finally, ice thickness was calculated from total thickness by subtracting the (interpolated) snow depths. GPS positions of snow depth and ice thickness measurements were subsequently corrected for ice drift using GPS recorders placed at the acoustic transponder locations to enable co-location with the transmittance measurements.

In addition, in situ snow depth, ice thickness, draft, freeboard, and melt pond depth were measured in drill holes at the marker locations using a tape measure on 17 August.

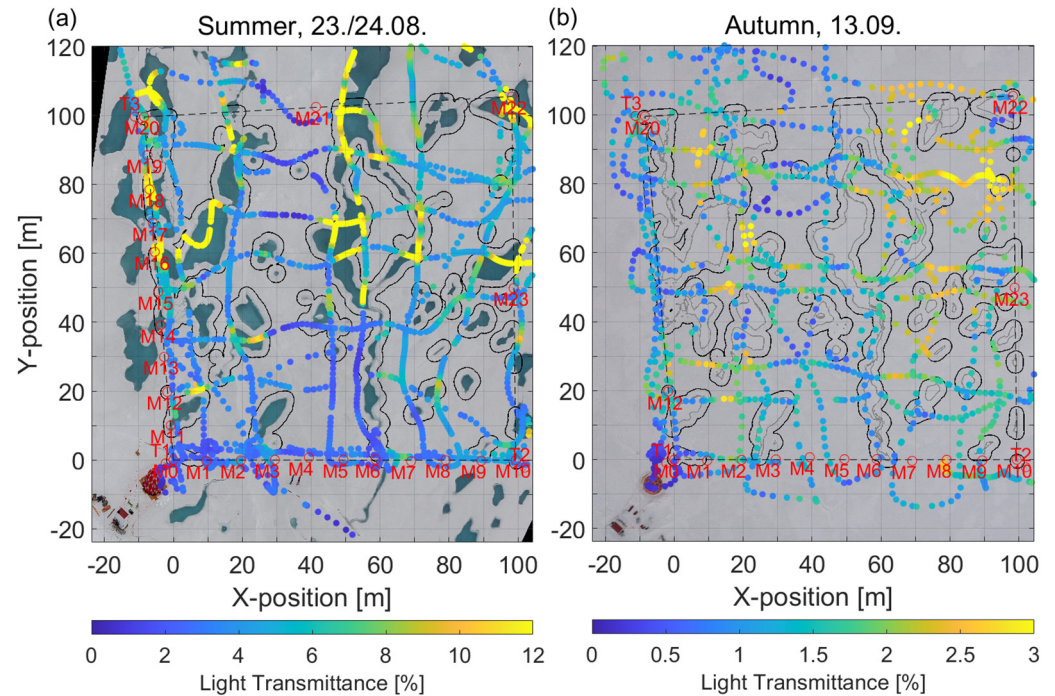


Figure 1. Distribution of melt ponds and bare ice on drifting MYI in the central Arctic during the transition from (a) summer to (b) autumn. The surfaces of the melt ponds were partly open and partly refrozen in (a) and completely refrozen and snow-covered in (b). Overlaid is light transmittance as measured using a remotely operated vehicle (ROV). The background images are orthorectified aerial images acquired during (a) a low altitude helicopter flight and (b) a drone flight. Pixels within the study area that were classified as melt ponds and used for further analysis are outlined by the melt ponds themselves in (a) and by the gray line in (b). The edges around the melt ponds in (a) and (b) were dilated by a buffer of about 2 m indicated by the black lines. Red labels indicate the marker (M) and transponder locations (T). The ROV tent and control hut are visible on the lower left corners of the images. Note the different ranges in transmittance in (a) and (b).

2.3. Under-Ice Transmittance

Horizontal transects of under-ice spectral irradiance were measured by a RAMSES-ACC hyper-spectral radiometer (TriOS GmbH, Rastede, Germany). The radiometer was mounted on a M500 ROV (Ocean Modules, Åtvidaberg, Sweden, Katlein et al., 2017). The ROV was lowered into the water through a 2×2 m hole in the ice covered by a tent next to the study area (Figure 1).

The light transmittance was calculated by wavelength-integrating the transmitted irradiance from 350 to 920 nm and normalizing by the incident downwelling planar irradiance recorded by an upward-looking reference sensor at the surface. The data were filtered for ROV pitch, roll, and depth, and the noise was filtered from the spectra. Using the photosynthetically active radiation (400–700 nm) did not lead to qualitatively different results and conclusions in this work, and is thus not further considered here.

For under-ice navigation, the ROV was equipped with an acoustic long baseline positioning system (Pinpoint 1500 Linkquest, San Diego, CA, USA). We manually post-processed the ROV position to remove distortions caused by calibration uncertainties.

2.4. Aerial Images

Oblique aerial images were obtained during a helicopter flight on 23 August (summer) and by a drone on 13 September (autumn). Those were used to retrieve the geographic coordinates of the melt ponds. The images were corrected for camera perspective and georeferenced using the marker locations measured by a terrestrial laser scanner (VZ-400i, RIEGL, Horn, Austria). Melt ponds in the image were detected using a simple threshold criterion. All pixels within the study area where $\text{mean}(R,G,B) < 70 + 0.5 \cdot B$ (Katlein et al., 2015) were classified as melt ponds, with R, G, B representing the integer values of the respective channels of the RGB color space

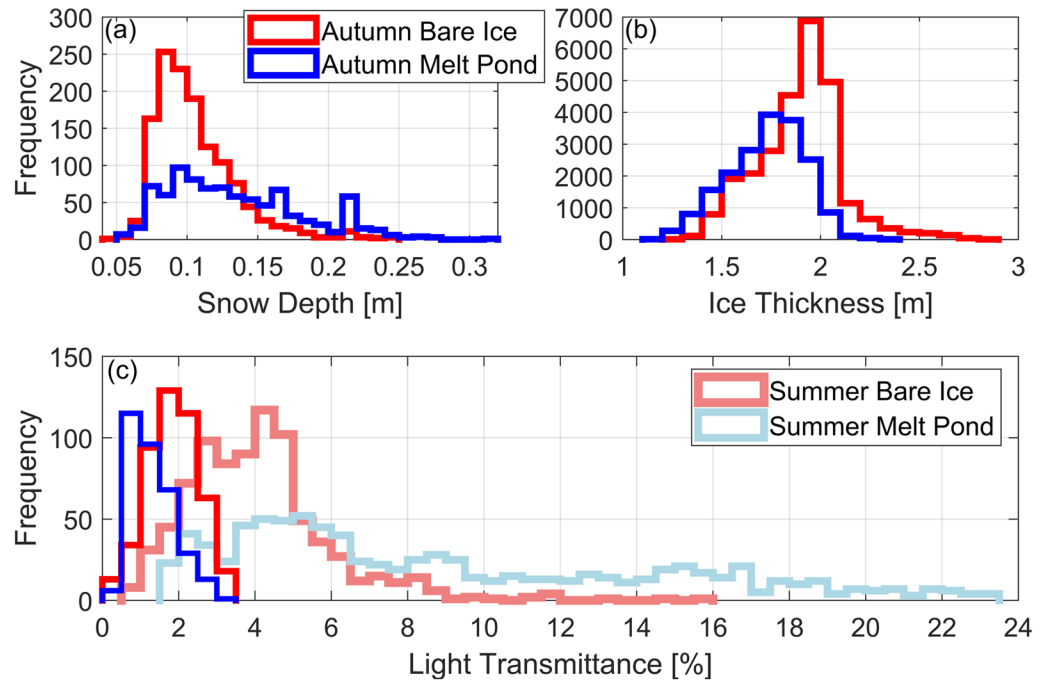


Figure 2. Histograms of measured (a) snow depth, (b) ice thickness, and (c) light transmittance of melt ponds and bare ice.

($R = 700$ nm, $G = 525$ nm, $B = 450$ nm). We added a 2 m buffer by image dilation to account for horizontal light spreading (Ehn et al., 2011) and uncertainties of the ROV position.

2.5. Radiative Transfer Model

We modeled broadband reflection and under-ice transmittance using the radiative transfer model DORT2002 version 3.0 (Edström, 2005; Katlein et al., 2021). The model uses a discrete ordinate model geometry and is implemented in the MATLAB™ software. The ice geometry was approximated by three layers each for bare ice and melt ponds (Table S1 in Supporting Information S1): The bare ice consisted of the interior sea ice underlying an SSL with a freshly fallen snow layer of varying thickness on top. The melt ponds consisted of interior sea ice underlying the melt pond overlain by a snow layer of varying thickness. For simplicity, the situation without any snow will be referred to as “summer” conditions whereas the snow-covered scenario is referred to as “autumn” conditions. We used typical inherent optical properties for multi-year ice (Katlein et al., 2021; Perron et al., 2021).

3. Results and Discussion

3.1. Evolution of the Snow Cover in the Transition From Summer to Autumn

Figure 1 illustrates the distribution of melt ponds and bare ice and their surface properties during the transition from summer to autumn in the study area.

On 23 August, the melt ponds were generally still open but in parts slightly refrozen at the surface (Figures 1a and S1 in Supporting Information S1). No significant snow fall occurred prior to 29 August (Vüllers et al., 2021), however, an SSL of deteriorated ice with a mean thickness of 0.07 m was present. The passage of low-pressure systems between 29 August and 15 September brought precipitation accompanied by strong winds with speeds up to 13 ms^{-1} (Vüllers et al., 2021). This wind speed exceeded the threshold of $8\text{--}10 \text{ ms}^{-1}$ under which divergence of large amounts of drifting snow is favorable (Van den Broeke & Bintanja, 1995). As a result, snow was deposited and re-distributed toward and caught by the recessed and refrozen melt ponds and their edges (Figure S1 in Supporting Information S1, Fetterer & Untersteiner, 1998; Perovich et al., 2003). This led to a higher mean snow accumulation on the ponds (0.14 m) compared to on bare ice (0.11 m) as measured on 13 September (Figure 2a,

Table S2 in Supporting Information S1). On the melt ponds, higher snow depths were also much more frequently measured than on bare ice (modes of 0.17 and 0.22 m, Figure 2a).

The snow mostly covered the visible surface signature of the ponds (Figure 1). However, the ponds were still discernible because of their brighter appearance due to the higher snow depth compared to the adjacent bare ice (Figure 1b).

The higher snow depth on the melt ponds can have important implications on the sea ice mass balance related to the insulating effect of the snow cover (Sturm et al., 1997). Reduced heat loss (Maykut, 1978) and thermodynamic ice growth (Maykut, 1978; Merkouriadi et al., 2017) as well as delayed freeze-up of the liquid melt pond (Flocco et al., 2015) and induced bottom roughness are expected.

The refrozen surface of the melt ponds alone reduces the heat release from the ocean through the ice toward the atmosphere (Flocco et al., 2015). This hampers ice growth at both water-ice interfaces of the refreezing pond, as well as between the sea ice bottom and the ocean in the transition from autumn to winter. This can result in a delay of the complete freeze-up of the pond by up to 60 days (Flocco et al., 2015). A thinner ice cover is more vulnerable to dynamic and warming events. The presence of a snow cover on top of the refrozen pond surface and the still liquid melt pond underneath are expected to amplify those effects (Perovich et al., 2003). As a result of the reduced thermodynamic growth of the sea ice underlying melt ponds compared to bare ice, a generally rougher bottom topography might result, affecting the mass, momentum, heat, and salt fluxes at the sea ice-ocean interface.

The exact evolution of the thicker snow cover on melt ponds during refreezing depends on the sequence of weather events. Whether or not more snow accumulates on the refrozen melt ponds than on adjacent bare ice is governed by the wind speed and snow drift regime during and after the snow fall, by the snow properties, and by the roughness of the refrozen surface. Falling and deposited snow needs to be re-distributed before it can accumulate on the topographically recessed and rougher pond surface. Wet and heavy snow is more resistant to erosion by wind than low-density dry snow (e.g., Colbeck, 1979; Massom et al., 1997). For instance, new snow deposited on blue ice either by drifting or precipitation can hardly settle on the smooth and warm surface (Bintanja, 1999; Van den Broeke & Bintanja, 1995). In case downwind slopes are smooth, any snow that can temporarily accumulate is prevented from actually attaching to the surface (Bintanja, 1999; Dacic et al., 2013). On such surfaces, drifting snow is also prevented from becoming attached causing the wind to be stronger over the glazed surface than over the snow (Frezzotti, Gandolfi, & Urbini, 2002). Furthermore, less snow will accumulate on smooth nilas with a low surface roughness (e.g., Massom et al., 1997; Sturm et al., 2002) than on surfaces with a higher surface roughness (e.g., Bintanja, 1999; Frezzotti, Gandolfi, La Marca, & Urbini, 2002).

3.2. Optical Properties

The surface topography of the ponded ice cover was key in modulating spatial variability in snow depth. The presence of open melt ponds in summer and the variability in snow depth driven by the refrozen melt ponds in autumn led to spatial and temporal variability in the under-ice light field. On 24 August, ROV-based mean and maximum transmittances of ponds (8.9% and 23.2%, respectively) were significantly higher than those of bare ice (4.1% and 15.5%, see also Figures 1a and 2c and Table S2 in Supporting Information S1). Histograms showed a bi-modal transmittance distribution of ponds and bare ice combined (Figure S2 in Supporting Information S1). The distribution also showed a characteristic long tail for ponds, indicating high spatial variability and different properties of the ponds. This distribution is typical for Arctic summer sea ice and results from the formation and development of the melt ponds (Katlein et al., 2015, 2019; Nicolaus et al., 2012; Schanke et al., 2021). The magnitudes of transmittance are similar to observations from Nicolaus et al. (2012) in the same region in August 2011. The maximum transmittance of the melt ponds also agrees to values found by Katlein et al. (2019).

Due to the new snow cover on top of both the refrozen melt ponds and the bare ice (Figure 1b), the transmittance of both melt ponds and bare ice decreased (Figures 1 and S2, Table S2 in Supporting Information S1). The spatial variability in the transmittance of both melt ponds and bare ice was significantly reduced in autumn while the long tail of the high transmittances diminished, with very few observations higher than 3% (Figures 2c and S2, Table S2 in Supporting Information S1). In summer, approximately 80% (25%) of the transmittance measurements were higher than 3% (9%). Due to stronger and more frequent snow fall events that started to occur from

28 August (Vüllers et al., 2021), only 1% (0%) of the transmittance measurements in autumn were higher than 3% (9%).

Lee et al. (2011) describe observations indicating that melt ponds remain bright windows even in autumn after refreezing, although they did not consider a snow cover. This implies that the transmittance of melt ponds remains higher than that of bare ice. Katlein et al. (2019) showed that the bi-modal structure of transmittance during summer is conserved even during the first weeks of freeze-up in mid of September. They further suggest that the transmittances of both melt ponds and bare ice decrease gradually and equally in the transition from summer to autumn. Snow and particularly re-distribution were observed during their transmittance measurements, however, the influences of the re-distribution on the transmittance were not investigated.

We observed a different scenario than Lee et al. (2011) and Katlein et al. (2019). A thicker snow cover accumulated on melt ponds compared to adjacent bare ice because of the recessed topography of the ponds. This led to a lower mean transmittance of melt ponds (1.3%) than of bare ice (1.8%) in autumn (Figures 1 and 2c, Table S2 in Supporting Information S1). The transmittance distribution showed two distinct modes of 1.0% and 2.0% associated with melt ponds and bare ice, respectively (Figures 2c and Table S2 in Supporting Information S1).

Despite the reversal of the magnitude in the transmittance of melt ponds and bare ice, the spatial variability remained during autumn (Figure 1). This suggests that the spatial variability was still coupled to the ponds after snow accumulation and re-distribution and most likely also persisted into winter.

The transmittance of ridged ice with thicknesses up to 2.8 m was naturally still lower than that of the melt ponds (Figures 1b and S3b in Supporting Information S1). Those measurements are included in the bare ice data and are represented in the tail of larger ice thicknesses in the histogram (Figure 2b).

This study provides quantitative observations of a thicker snow cover on melt ponds than on adjacent bare ice in autumn. Besides lower light transmittance of melt ponds than of bare ice due to higher snow depths on the ponds, major implications on the ice-associated ecosystem and the energy balance of the sea ice might arise from those observations in case such a situation is viable for the entire Arctic which is very likely.

Lee et al. (2011) proposed that the soft refrozen surface of open melt ponds that are in connection with the ocean provides a fertile habitat for biomass in autumn. They pointed out that the biomass accumulated under the refrozen melt ponds serves as an important food source for higher trophic animals during the transition from autumn to winter and further into winter. However, as presented here, a snow cover significantly reduces the light availability in and under melt ponds in autumn, suggesting limited suitability as a habitat in terms of available light. These observations lend support to a study by Lange et al. (2017), who found higher biomass values underneath hummocks on multi-year ice compared to adjacent level ice. Lange et al. (2017) attributed the differences in biomass accumulation to increased light availability under the hummocks resulting from a very thin or absent snow cover (Perovich et al., 2003). Our results and those of Lange et al. (2017) suggest that light conditions under sea ice in spring can already be initialized by melt pond coverage and snow distribution during autumn and may persist throughout winter.

Further, due to the common assumption that there is more light available under melt ponds than under bare ice also during autumn, processes and magnitudes of carbon uptake and biomass accumulation in models, might need to be adjusted with respect to our new observations.

Arndt and Nicolaus (2014) developed a parameterization to quantify the annual solar heat input through Arctic sea ice. For their calculations in autumn, they use for transmittances of melt ponds the fivefold (500%) of that of bare ice. However, our results showed that the modal transmittance of melt ponds is only half (50%) of that of bare ice once covered by the first snow (Table S2 in Supporting Information S1). Arndt and Nicolaus (2014) applied a constant summer mean melt pond fraction for multi-year ice of 29% (Rösel et al., 2012) and transmittance of melt ponds for multi-year ice of 0.4%. They estimated the solar heat input into the ocean in September to 0.69×10^{19} J. We adopted their parameters but used the ratio of transmittances between melt ponds and bare ice as presented in the present study. As a result, the solar heat input into the ocean decreased by 61%. This shows, that despite the generally low solar energy fluxes in autumn compared to in summer (e.g., Arndt & Nicolaus, 2014; Perovich et al., 2011), our described effect could have an important impact on the energy budget if valid in the entire Arctic. In this regard, our results might also impact the heat stored in the upper ocean, the interior sea ice structure, as well as internal and basal melting.

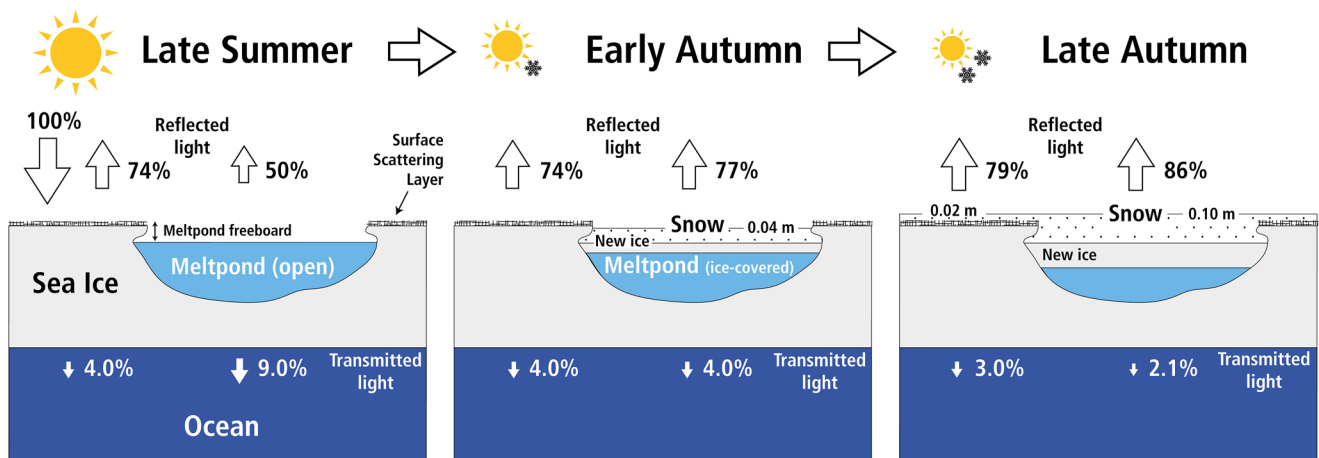


Figure 3. A bright window turns into a dark spot: graphical representation of the situation observed in this study. During the transition from summer to autumn, snow predominantly accumulated on the recessed surface of frozen melt ponds, resulting in a reversal of the light transmittance between melt ponds and bare ice. Numbers result from the radiative transfer model DORT2002. Properties used in the model are displayed in Table S1 in Supporting Information S1.

3.3. Radiative Transfer Model

For the effect described above, it is of interest to quantify the threshold snow depth that is necessary to decrease the transmittance of melt ponds below that of bare ice for the specific environmental conditions we have observed (Table S1 in Supporting Information S1). To determine this threshold depth, we used the radiative transfer model DORT2002. Figure 3 summarizes the observations of this study as a schematic which is supported by simulated albedo and transmittance. For the situation without snow (summer), both the simulated transmittances of melt ponds and bare ice (9% and 4%, respectively) were very similar to our observations (8.9% and 4.1%, respectively, Figures 3 and S4, Table S2 in Supporting Information S1).

Incorporating an increasing snow cover from 0 to 0.20 m (autumn), our results yielded an exponential decrease in the transmittances of both melt ponds and bare ice (Figure S4 in Supporting Information S1). For a snow depth of approximately 0.04 m, the transmittance of the melt ponds becomes equal to that of snow-free bare ice for this specific situation (Figures 3 and S4 in Supporting Information S1). This is in agreement with the observations which showed that the transmittance of melt ponds was lower than that of bare ice for a 0.03 m higher mean snow depth on the ponds (Table S2 in Supporting Information S1). Figure 3 illustrates that the transmittance of melt ponds with a 0.10 m thick snow cover is significantly lower than that of bare ice with a 0.02 m thick snow cover.

In our simulations, the influence of the thin ice lid on the melt ponds on the transmittance was neglected, as they were only partially existing, as for typical Arctic summer sea ice these are very translucent and scattering is small (Lu et al., 2018), indicated by their blue-green color (Figure 1a).

4. Summary

Snow depth measurements on a ponded sea-ice floe in the transition from summer to autumn reveal that snow accumulation was on average 0.03 m higher on refrozen melt ponds than on adjacent bare ice favored by the recessed topography of the ponds. Using under-ice radiation measurements from an ROV we show that due to the thicker snow cover on the melt ponds the transmittance of the melt ponds can become lower than that of bare ice. Those results imply that melt ponds cannot be universally considered as bright windows of Arctic autumn sea ice. This finding is supported by computations from a radiative transfer model. Our findings can have consequences for the autumn ecosystem activity, oceanic heat budget, and thermodynamic ice growth if they can be observed in the entire Arctic.

Conflict of Interest

The authors declare no conflicts of interest relevant to this study.

Data Availability Statement

All data presented in this study are publicly available under the following DOIs: ROV: [doi:10.1594/PAN-GAEA.925698](https://doi.org/10.1594/PAN-GAEA.925698), Magna Probe and GEM2: [doi:10.1594/PANGAEA.934431](https://doi.org/10.1594/PANGAEA.934431), Aerial images: [doi:10.5281/zenodo.5119094](https://doi.org/10.5281/zenodo.5119094).

Acknowledgments

We thank the editor Harihar Rajaram and two anonymous reviewers for improving this work. This work was financed through the research programs PACES II and POF4 of the Alfred-Wegener-Institut Helmholtz-Zentrum für Polar- und Meeresforschung (AWI) and the Swedish Polar Research Secretariat (SPRS, grant no. AO18). Additional funding was received through the Diatom-ARCTIC project (NE/R012849/1; 03F0810A) as part of the Changing Arctic Ocean program (CAO), jointly funded by the UKRI Natural Environment Research Council (NERC) and the German Federal Ministry of Education and Research (BMBF). The ROV work was supported by the Helmholtz Infrastructure Initiative “Frontiers in Arctic marine Monitoring” (FRAM). We are thankful to the captain, crew and scientists onboard the *IB Oden*, as well as to the SPRS and AWI logistics for facilitating our participation in the AO18 expedition. Our special thanks go to Matthieu Labaste, Helen Czerski, and Lars Lehnert for their field support, Ruzica Dadić for her advice on snow, and the polar bear guarding crew for keeping us safe. We also acknowledge financial support by the Open Access Publication Funds of AWI.

References

- Ardyna, M., Mundy, C. J., Mills, M. M., Oziel, L., Grondin, P.-L., Lacour, L., et al. (2020). Environmental drivers of under-ice phytoplankton bloom dynamics in the Arctic Ocean. *Elementa: Science of the Anthropocene*, 8(30). <https://doi.org/10.1525/elementa.430>
- Arndt, S., & Nicolaus, M. (2014). Seasonal cycle and long-term trend of solar energy fluxes through Arctic sea ice. *The Cryosphere*, 8(6), 2219–2233. <https://doi.org/10.5194/tc-8-2219-2014>
- Arrigo, K. R. (2014). Sea ice ecosystems. *Annual Review of Marine Science*, 6(1), 439–467. <https://doi.org/10.1146/annurev-marine-010213-135103>
- Bintanja, R. (1999). On the glaciological, meteorological, and climatological significance of Antarctic blue ice areas. *Reviews of Geophysics*, 37(3), 337–359. <https://doi.org/10.1029/1999rg900007>
- Colbeck, S. C. (1979). Sintering and compaction of snow containing liquid water. *Philosophical Magazine A*, 39(1). <https://doi.org/10.1080/01418617908239272>
- Dadić, R., Mott, R., Horgan, H. J., & Lehning, M. (2013). Observations, theory, and modeling of the differential accumulation of Antarctic megadunes. *Journal of Geophysical Research: Earth Surface*, 118(4), 2343–2353. <https://doi.org/10.1002/2013jf002844>
- Edström, P. (2005). A Fast and Stable Solution Method for the Radiative Transfer Problem. *Society for Industrial and Applied Mathematics Review*, 47(3), 447–468. <https://doi.org/10.1137/s0036144503438718>
- Ehn, J. K., Mundy, C. J., Barber, D. G., Hop, H., Rossnagel, A., & Stewart, J. (2011). Impact of horizontal spreading on light propagation in melt pond covered seasonal sea ice in the Canadian Arctic. *Journal of Geophysical Research*, 116. <https://doi.org/10.1029/2010jg006908>
- Fetterer, F., & Untersteiner, N. (1998). Observations of melt ponds on Arctic sea ice. *Journal of Geophysical Research*, 103(C11), 24821–24835. <https://doi.org/10.1029/98jc02034>
- Flocco, D., Feltham, D. L., Bailey, E., & Schroeder, D. (2015). The refreezing of melt ponds on Arctic sea ice. *Journal of Geophysical Research: Oceans*, 120(2), 647–659. <https://doi.org/10.1002/2014jc010140>
- Frezzotti, M., Gandolfi, S., La Marca, F., & Urbini, S. (2002). Snow dunes and glazed surfaces in Antarctica: New field and remote-sensing data. *Annals of Glaciology*, 34, 81–88. <https://doi.org/10.3189/172756402781817851>
- Frezzotti, M., Gandolfi, S., & Urbini, S. (2002). Snow megadunes in Antarctica: Sedimentary structure and genesis. *Journal of Geophysical Research*, 107(D18). <https://doi.org/10.1029/2001jd000673>
- Grenfell, T. C., & Maykut, G. A. (1977). The optical properties of ice and snow in the Arctic Basin. *Journal of Glaciology*, 18(80). <https://doi.org/10.3189/S0022143000021122>
- Hanson, A. (1965). Studies of the Mass Budget of Arctic Pack-Ice Floes. *Journal of Glaciology*, 5(41). <https://doi.org/10.3189/S0022143000018694>
- Horvat, C., Jones, D. R., Iams, S., Schroeder, D., Flocco, D., & Feltham, D. (2017). The frequency and extent of sub-ice phytoplankton blooms in the Arctic Ocean. *Science Advances*, 3(3). <https://doi.org/10.1126/sciadv.1601191>
- Hunkeler, P. A. (2016). *Sea-ice thickness and porosity from multi-frequency electromagnetic induction sounding: Application to the sub-ice platelet layer in Atka Bay, Antarctica*, PhD thesis (p. 10013). Jacobs University Bremen.
- Hunkeler, P. A., Hoppmann, M., Hendricks, S., Kalscheuer, T., & Gerdes, R. (2016). A glimpse beneath Antarctic sea ice: Platelet layer volume from multifrequency electromagnetic induction sounding. *Geophysical Research Letters*, 43(1), 222–231. <https://doi.org/10.1002/2015gl065074>
- Katlein, C., Arndt, S., Belter, H. J., Castellani, G., & Nicolaus, M. (2019). Seasonal evolution of light transmission distributions through Arctic Sea Ice. *Journal of Geophysical Research: Oceans*, 124(8), 5418–5435. <https://doi.org/10.1029/2018jc014833>
- Katlein, C., Arndt, S., Nicolaus, M., Perovich, D. K., Jakuba, M. V., Suman, S., et al. (2015). Influence of ice thickness and surface properties on light transmission through Arctic sea ice. *Journal of Geophysical Research: Oceans*, 120(9), 5932–5944. <https://doi.org/10.1002/2015JC010914>
- Katlein, C., Schiller, M., Belter, H. J., Coppolaro, V., Wenslandt, D., & Nicolaus, M. (2017). A New Remotely Operated Sensor Platform for Interdisciplinary Observations under Sea Ice. *Frontiers in Marine Science*, 4. <https://doi.org/10.3389/fmars.2017.00281>
- Katlein, C., Valcic, L., Lambert-Girard, S., & Hoppmann, M. (2021). New insights into radiative transfer within sea ice derived from autonomous optical propagation measurements. *The Cryosphere*, 15(1), 183–198. <https://doi.org/10.5194/tc-15-183-2021>
- Lange, B. A., Flores, H., Michel, C., Beckers, J. F., Bublit, A., Casey, J. A., et al. (2017). Pan-Arctic sea ice-algal chl a biomass and suitable habitat are largely underestimated for multiyear ice. *Global Change Biology*, 23(11), 4581–4597. <https://doi.org/10.1111/gcb.13742>
- Lee, S. H., McRoy, C. P., Joo, H. M., Gradinger, R., Cui, H., Yun, M. S., et al. (2011). Holes in progressively thinning Arctic sea ice lead to new ice algae habitat. *Oceanography*, 24(3), 302–308. <https://doi.org/10.5670/oceanog.2011.81>
- Light, B., Grenfell, T. C., & Perovich, D. K. (2008). Transmission and absorption of solar radiation by Arctic sea ice during the melt season. *Journal of Geophysical Research*, 113, C03023. <https://doi.org/10.1029/2006jc003977>
- Light, B., Perovich, D. K., Webster, M. A., Polashenski, C., & Dadić, R. (2015). Optical properties of melting first-year Arctic sea ice. *Journal of Geophysical Research: Oceans*, 120(11), 7657–7675. <https://doi.org/10.1002/2015jc011163>
- Lu, P., Cao, X., Wang, Q., Leppäranta, M., Cheng, B., & Li, Z. (2018). Impact of a surface ice lid on the optical properties of melt ponds. *Journal of Geophysical Research: Oceans*, 123(11), 8313–8328. <https://doi.org/10.1029/2018jc014161>
- Massom, R. A., Drinkwater, M. R., & Haas, C. (1997). Winter snow cover on sea ice in the Weddell Sea. *Journal of Geophysical Research*, 102(C1), 1101–1117. <https://doi.org/10.1029/96jc02992>
- Maykut, G. A. (1978). Energy exchange over young sea ice in the central Arctic. *Journal of Geophysical Research*, 83(C7), 3646. <https://doi.org/10.1029/JC083iC07p03646>
- Merkouriadi, I., Cheng, B., Graham, R. M., Rösel, A., & Granskog, M. A. (2017). Critical role of snow on sea ice growth in the Atlantic Sector of the Arctic Ocean. *Geophysical Research Letters*, 44(20), 479–510. <https://doi.org/10.1002/2017gl075494>
- Nicolaus, M., Katlein, C., Maslanik, J., & Hendricks, S. (2012). Changes in Arctic sea ice result in increasing light transmittance and absorption. *Geophysical Research Letters*, 39(24). <https://doi.org/10.1029/2012gl053738>
- Perovich, D. K., Grenfell, T. C., Light, B., Elder, B. C., Harbeck, J. P., Polashenski, C., et al. (2009). Transpolar observations of the morphological properties of Arctic sea ice. *Journal of Geophysical Research*, 114, C00A04. <https://doi.org/10.1029/2008jc004892>
- Perovich, D. K., Grenfell, T. C., Richter-Menge, J. A., Light, B., Tucker III, W. B., & Eicken, H. (2003). Thin and thinner: Sea ice mass balance measurements during SHEBA. *Journal of Geophysical Research*, 108(C3). <https://doi.org/10.1029/2001jc001079>

- Perovich, D. K., Richter-Menge, J. A., Jones, K. F., Light, B., Elder, B. C., Polashenski, C., et al. (2011). Arctic sea-ice melt in 2008 and the role of solar heating. *Annals of Glaciology*, 52(57). <https://doi.org/10.3189/172756411795931714>
- Perovich, D. K., Tucker III, W. B., & Ligett, K. A. (2002). Aerial observations of the evolution of ice surface conditions during summer. *Journal of Geophysical Research*, 107(C10). <https://doi.org/10.1029/2000jc000449>
- Perron, C., Katlein, C., Lambert-Girard, S., Leymarie, E., Guinard, L.-P., Marquet, P., & Babin, M. (2021). Development of a diffuse reflectance probe for in situ measurement of inherent optical properties in sea ice. *The Cryosphere*, 15(9), 4483–4500. <https://doi.org/10.5194/tc-15-4483-2021>
- Petrich, C., Eicken, H., Polashenski, C. M., Sturm, M., Harbeck, J. P., Perovich, D. K., & Finnegan, D. C. (2012). Snow dunes: A controlling factor of melt pond distribution on Arctic sea ice. *Journal of Geophysical Research: Oceans*, 117, C09029. <https://doi.org/10.1029/2012jc008192>
- Polashenski, C., Perovich, D. K., & Courville, Z. (2012). The mechanisms of sea ice melt pond formation and evolution. *Journal of Geophysical Research*, 117(C1). <https://doi.org/10.1029/2011jc007231>
- Rösel, A., Kaleschke, L., & Birnbaum, G. (2012). Melt ponds on Arctic sea ice determined from MODIS satellite data using an artificial neural network. *The Cryosphere*, 6(2), 431–446. <https://doi.org/10.5194/tc-6-431-2012>
- Schanke, N. L., Bolinesi, F., Mangoni, O., Katlein, C., Anhaus, P., Hoppmann, M., et al. (2021). Biogeochemical and ecological variability during the late summer–early autumn transition at an ice-floe drift station in the Central Arctic Ocean. *Limnology & Oceanography*, 66(S1). <https://doi.org/10.1002/lno.11676>
- Schröder, D., Feltham, D. L., Flocco, D., & Tsamados, M. (2014). September Arctic sea-ice minimum predicted by spring melt-pond fraction. *Nature Climate Change*, 4(5), 353–357. <https://doi.org/10.1038/nclimate2203>
- Sturm, M., & Holmgren, J. (2018). An automatic snow depth probe for field validation campaigns. *Water Resources Research*, 54(11), 9695–9701. <https://doi.org/10.1029/2018wr023559>
- Sturm, M., Holmgren, J., König, M., & Morris, K. (1997). The thermal conductivity of seasonal snow. *Journal of Glaciology*, 43(143), 26–41. <https://doi.org/10.3189/S002214300002781>
- Sturm, M., Holmgren, J., & Perovich, D. K. (2002). Winter snow cover on the sea ice of the Arctic Ocean at the surface heat budget of the Arctic Ocean (SHEBA): Temporal evolution and spatial variability. *Journal of Geophysical Research*, 107(C10). <https://doi.org/10.1029/2000jc000400>
- Untersteiner, N. (1961). On the mass and heat budget of arctic sea ice. *Archiv für Meteorologie, Geophysik und Bioklimatologie, Serie A*, 12, 151–182. <https://doi.org/10.1007/BF02247491>
- van den Broeke, M. R., & Bintanja, R. (1995). Summertime atmospheric circulation in the vicinity of a blue ice area in Queen Maud Land, Antarctica. *Boundary-Layer Meteorology*, 72, 411–438. <https://doi.org/10.1007/BF00709002>
- Vüllers, J., Achtert, P., Brooks, I. M., Tjernström, M., Prytherch, J., Burzik, A., & Neely III, R. (2021). Meteorological and cloud conditions during the Arctic Ocean 2018 expedition. *Atmospheric Chemistry and Physics*, 21(1), 289–314. <https://doi.org/10.5194/acp-21-289-2021>
- Webster, M., Gerland, S., Holland, M., Hunke, E., Kwok, R., Lecomte, O., et al. (2018). Snow in the changing sea-ice systems. *Nature Climate Change*, 8, 946–953. <https://doi.org/10.1038/s41558-018-0286-7>
- Webster, M. A., Rigor, I. G., Nghiem, S. V., Kurtz, N. T., Farrell, S. L., Perovich, D. K., & Sturm, M. (2014). Interdecadal changes in snow depth on Arctic sea ice. *Journal of Geophysical Research: Oceans*, 119(8), 5395–5406. <https://doi.org/10.1002/2014jc009985>
- Webster, M. A., Rigor, I. G., Perovich, D. K., Richter-Menge, J. A., Polashenski, C. M., & Light, B. (2015). Seasonal evolution of melt ponds on Arctic sea ice. *Journal of Geophysical Research: Oceans*, 120(9), 5968–5982. <https://doi.org/10.1002/2015jc011030>

References From the Supporting Information

- Ehn, J. K., Papakyriakou, T. N., & Barber, D. G. (2008). Inference of optical properties from radiation profiles within melting landfast sea ice. *Journal of Geophysical Research*, 113, C09024. <https://doi.org/10.1029/2007jc004656>
- Perovich, D. K. (1990). Theoretical estimates of light reflection and transmission by spatially complex and temporally varying sea ice covers. *Journal of Geophysical Research*, 95(C6), 9557. <https://doi.org/10.1029/JC095iC06p09557>
- Petrich, C., Nicolaus, M., & Gradinger, R. (2012). Sensitivity of the light field under sea ice to spatially inhomogeneous optical properties and incident light assessed with three-dimensional Monte Carlo radiative transfer simulations. *Cold Regions Science and Technology*, 73, 1–11. <https://doi.org/10.1016/j.coldregions.2011.12.004>